Creation Research Society Quarterly 2023 59:151–159

Baraminic Placement of *Homo heidelbergensis* Based on Molecular Data

Matthew Cserhati

Abstract

The consensus of creationist opinion places *Homo heidelbergensis* within the human holobaramin. This is based on morphological data, but what do the molecular data say? Can we build a stronger holistic case for this fossil by adding molecular data? Further evidence for the humanity of *Homo heidelbergensis* comes from the sequence analysis of the mitochondrial genome of several dozen primate species. Nuclear data has also been isolated from *Homo heidelbergensis* fossils from Sima de los Huesos. These sequencing reads and sequencing data from an archaic ("Paleolithic") human were mapped to the genomes of modern human, Neanderthal, and chimpanzee. Based on the proportion of mapping reads and the sequence similarity of these reads when mapped to the human genome, *Homo heidelbergensis* can confidently be placed in the human holobaramin. Both morphological and genetic evidence additively support this conclusion.

Key Words: *Homo heidelbergensis*, Neanderthal, modern humans, *Pan*, mitochondrial DNA, variant analysis

Introduction

In general, the fossil hominid *Homo heidelbergensis* is taken by creationists to be a member of the human holobaramin (Woodmorappe, 1999; Lubenow, 2004; Line, 2013; Rupe and Sanford, 2017). The holobaramin is defined as the complete species membership of a given kind. They do this based on their more *erectus*-like features (Line, 2013). *Homo erectus* has generally been accepted by most creationists as human. Even some evolutionists (e.g., Wood and Collard, 1999) note the human-like body size, locomotion, jaws, and teeth of *H. heidelbergensis*. For example, the cranial capacity of *H. heidelbergensis* specimen Kabwe 1, is 1325 cc, which fits within the lower range of modern humans.

The sequencing of the mitochondrial DNA (mtDNA) (Meyer et al., 2014) and the availability of Next-Generation sequencing reads have made the molecular analysis of *H. heidelbergensis* possible. This is great news for creationists, since molecular evidence may possibly re-affirm the baraminic status of *H. heidelbergensis*.

The mtDNA sequence similarity between *H. heidelbergensis* and other primates has already been analyzed (Cserhati, 2022). *H. heidelbergensis* was shown to fall within the human holobaramin.

Furthermore, read sequences derive from ancient DNA (aDNA) from *H.*

Accepted for publication May 16, 2022

heidelbergensis can also be aligned to the whole genome sequence (WGS) of modern human and *Pan troglodytes* to examine how well these reads match to the two genomes. The proportion of aligned reads, the number of single nucleotide polymorphisms (SNPs), and the mean read sequence similarity could be used to get a broad picture of how *H. heidelbergensis* is related or not to modern humans and chimpanzee.

Materials and Methods

Data sets

A list of NCBI accession numbers for the mtDNA sequences of 36 primates and the South American gray short-tailed possum (*Monodelphis domestica*) is available in Supplementary File 1. The 28 *Homo* and 3 *Pan* NCBI accessions can be found in Supplementary File 2. From the second data set, *Homo sapiens* isolate NA24143 and NA24149 and EgyprRef1 were recoded into their reverse complement sequence so they could be used in further analysis.

In a second study comparing the sequence similarity of *H. heidelbergensis* with human, 21 mtDNA sequences from modern humans were downloaded from NCBI together with one from Neanderthal, Denisovan, and *H. heidelbergenesis*, respectively, and two mtDNA sequences

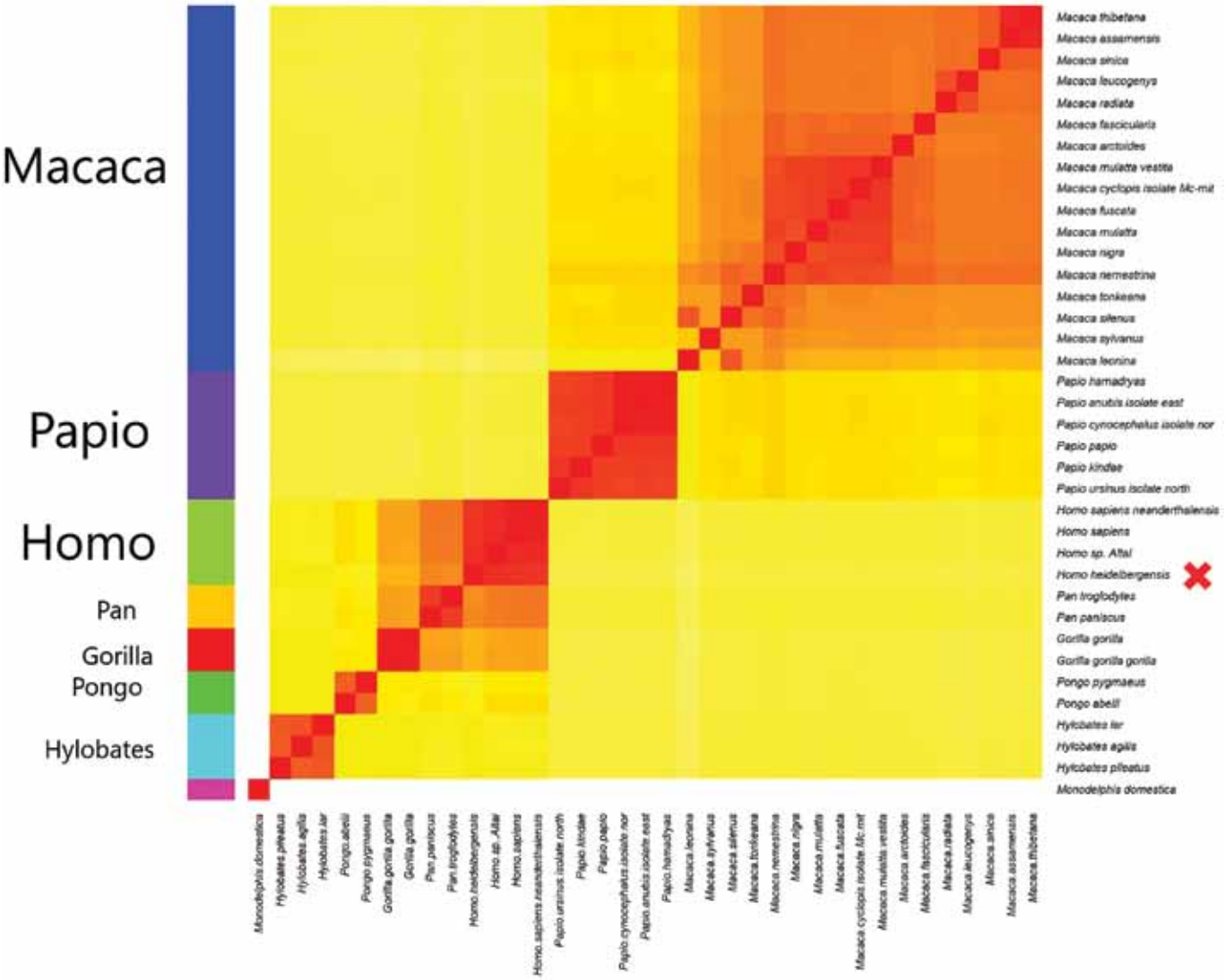

Figure 1. Heatmap showing hierarchical species relationships between 36 primate species as well as the outlier *Monodelphis domestica*. The heatmap depicts sequence mtDNA similarity values between all pairs of species in the analysis. Lighter colors denote higher similarity values between species which are closer relatives, whereas darker colors denote lower similarity values. *H. heidelbergenesis* is denoted with a red "X."

from *Pan paniscus* and one from *P. troglodytes*.

Nine *H. heidelbergensis* Sequence Read Archive (SRA) data sets from BioProject PRJEB10597 and ten SRA data sets from archaic (so-called "Paleolithic") humans from BioProject PRJEB22592 were aligned to the hg38 WGS of modern human and the panTrog6 (or pt6) WGS of *P. troglodytes* (Sikora et al., 2017). These genomes were downloaded from the UCSC browser, whereas the Neanderthal WGS was downloaded from the website of the Bioinformatics Core of UNMC (University of Nebraska Medical Center). A bowtie2 index was created for all three WGS using the bowtie2-index command. The vcf file containing 1,112,554,591 SNPs from the dbSNP database was downloaded from ftp.ncbi.nih.gov/snp/latest_release/VCF/GCF_000001405.39.gz.

The SRA data sets for PRJEB10597 are listed in Supplementary File 3, along with the number of reads in each data set and several statistics calculated during the analysis. The SRA data sets and the results for PRJEB22592 are listed in Supplementary File 4. All Supplementary files are available on Zenodo at https://zenodo.org/record/6551642#.YoF8q1TMLrc.

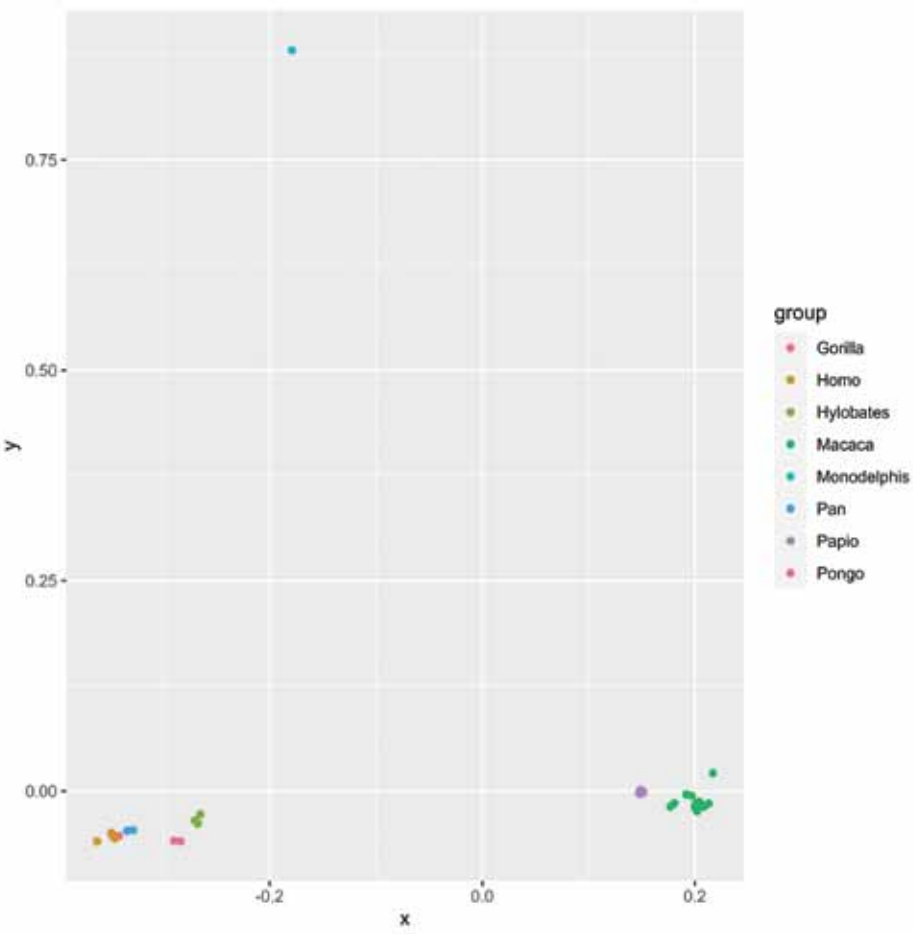

Figure 2. Two-dimensional MDS plot of 36 primate species plus *M. domestica* as an outlier. Eight disjunct groups can be observed, each represented by a separate color, as seen in the color legend.

Generation of plots

For the generation of the heatmap (Figure 1) showing the baraminic relationships between the 36 primate species and the outlier, the heatmap.2 function using the 'single' clustering method was used. The MDS plot in Figure 2 was created using the cmdscale function to create MDS plot coordinates. Figure 3 was created using the hist function in R, and Figure 5 was created using the plot function. The MEGA-X software (Kumar et al., 2018) was used to create alignments for the mtDNA for the 28 human mtDNA sequences and the baraminic tree in Figure 4 using the Neighbor Joining method (Saitou and Nei, 1987; Tamura et al., 2004). Default parameters were used to generate the tree. Supplementary Figures 1a and 1b were generated using the treemap tool in R.

Data processing pipeline

When aligning the archaic reads from *H. heidelbergensis*, the bowtie2 aligner was used against bwa-mem, since bowtie2 is faster and increases genome coverage when aligning aDNA reads (Poullet and Orlando, 2020). The bowtie2 aligner was run with the —local and —end-to-end flags. The bwa aligner was not used due to the fact that it presumes that there are few differences between the query and the target sequence within the first 32 bp, which frequently is the case with aDNA (Schubert et al., 2014). The resulting sam files were transformed into bam files and sorted for the mpileup function of samtools. Finally, for each sample, variants were called using bcftools with the following command: bcftools call -P 1e-3 -mv -Ob. The -P flag means that variants were called at a p-value of 0.001.

For each sample, the number of reads and the proportion of reads aligning to hg38 and pt6 were noted in separate columns in Supplementary Files 3 and 4. Then, the variant density

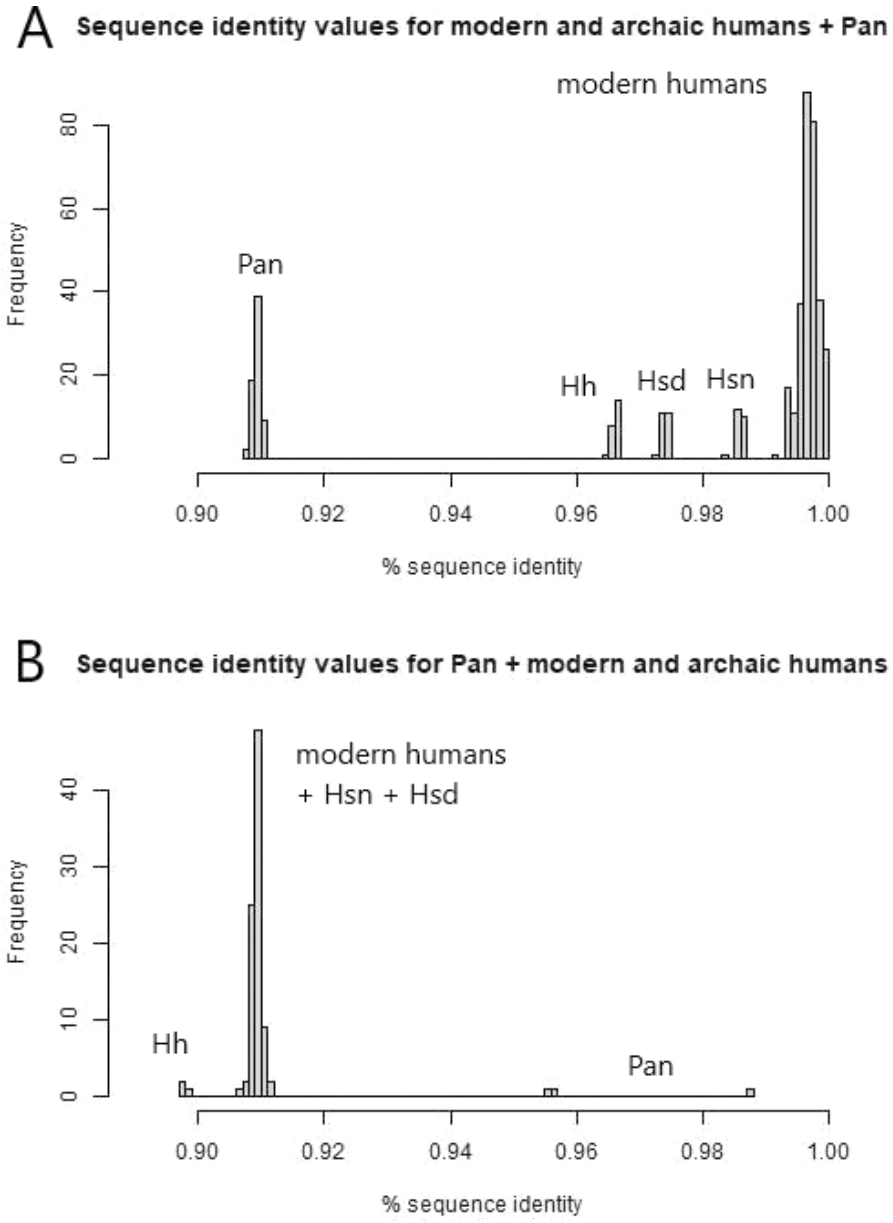

Figure 3. (A.) Histogram showing frequencies of mtDNA sequence similarity values, shown on the x-axis. The sequence similarity values between *Pan*, *H. heidelbergensis* (Hh), Denisova (Hsd), Neanderthal (Hsn), and modern humans are depicted compared to modern humans. (B.) Histogram showing frequencies of mtDNA sequence similarity values, shown on the x-axis. The sequence similarity values between *H. heidelbergensis* (Hh), Denisova (Hsd), Neanderthal (Hsn), modern humans, and *Pan* are depicted compared to *Pan*.

was calculated for hg38 and pt6 WGS by dividing the number of reads by the number of variants found for that sample. Next, the hg38/pt6 density proportion was calculated by dividing the variant density of pt6 with the variant density of hg38 to see whether there are more variants in the *P. troglodytes* genome compared to human.

The variant calling pipeline was run on an Ubuntu 18.04.1 operating system. Student's t-tests were run in R, version 4.1.0. using the t.test command. Two t-tests were run to calculate the p-values reported in Table 4: a normal t-test and a second one where the 'alternative' parameter was set to 'less.' This is because the values in the first data set are less than those in the second data set used in the t-test.

Read sequence similarity analysis

For each sample from PRJEB10957 and PRJEB22952, the first 10,000 reads from the fastq file were converted to fasta files using the fastq_to_fasta tool. They were then BLASTed against the hg38 and pt6 genomes using blastn. Z-scores were calculated to tell how statistically significantly similar two normal distributions were, based on the following equation:

$$Z = \frac{(\bar{X}_1 - \bar{X}_2)}{\sqrt{\sigma^2_{\bar{X}_1} + \sigma^2_{\bar{X}_2}}}$$

where $\bar{X}_1$ and $\bar{X}_2$ stand for the mean value of both distributions, and $\sigma^2_{\bar{X}_1}$, $\sigma^2_{\bar{X}_2}$ stands for the standard deviation.

Results and Discussion

Mitochondrial DNA sequence similarity

The result of the alignment of the 36 primate mtDNA sequences can be seen in the heatmap in Figure 1. The South American gray short-tailed possum (*Monodelphis domestica*) was used as an outlier). The Hopkins clustering statistic is 0.904, which indicates very good clustering. The species visibly form compact clusters. Based on k-means clustering, there are seven clusters corresponding to the seven primate genera selected for the study. *H. heidelbergensis*, *H. sapiens*, Neanderthal, and Denisovan form a cluster.

The mean sequence identity value between all four species in this cluster is 97.33±0.77% (p-value = $2.5x10^{-30}$). In contrast, the mean sequence similarity between the four *Homo* individuals with *Pan paniscus* and *P. troglodytes* is 90.7±0.58%. This is quite different from the long-held 99% genetic similarity between chimpanzees and humans and is in line with the work of Tomkins (Tomkins, 2015, 2018).

In contrast to these alignments using short reads, Tomkins reported that the mean similarity of BLASTN alignments with 18,000 long-read de novo assembled sequencing contigs of chimpanzee genomic DNA queried onto the human genome was only 84% (Tomkins, 2018). In Tomkins' analysis, the contigs on average were about 30,913 bases in length, but the achieved alignments were only on average 10,508 bases in length due to regions of dissimilarity that could not be bridged despite the liberal gap extension parameters that were used. Thus, the actual genome-wide similarity between chimps and humans may prove to be even lower. The results from the present study and previous work by Tomkins are quite different from the long-held myth of 99% genetic similarity between chimpanzees and humans.

In the MDS plot in Figure 2, the seven groups (plus *M. domestica* as an outlier) are coded with different colored dots. To the lower left, we have *Homo*, *Gorilla*, *Pan*, *Hylobates*, and *Pongo*. To the lower right, we have *Macaca* and *Papio*. The outlier, *M. domestica*, is at the center top of the plot. The MDS coordinates for all 37 species are provided in Supplementary File 1.

In Figure 3, two histograms showing the frequencies of mtDNA sequence similarities (MSS) are shown. In Figure 3A, we see the frequency of MSS between 21 modern humans and among modern humans and Neanderthal, Denisovan, *H. heidelbergensis*, and *Pan*. *H. heidelbergensis* is arguably the least similar archaic human compared to modern humans. It is the farthest away from modern humans, followed by Denisovan and then Neanderthal. This is to be expected, since *H. heidelbergensis* is the oldest individual from the *Homo* group, being a super-archaic human.

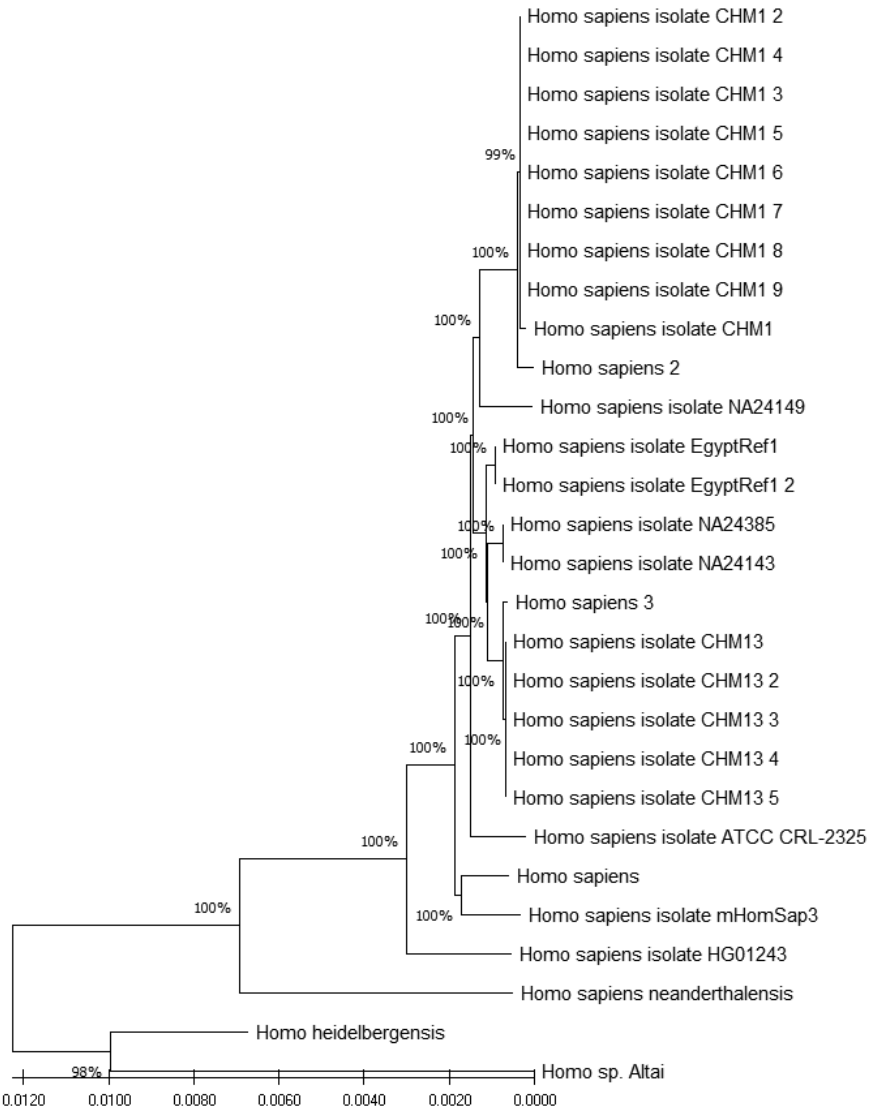

Figure 4. Baraminic tree produced by MEGA-X based on the Neighbour-Joining method. The software used the multiple alignments of 28 modern and archaic human mtDNA sequences.

However, in Figure 3B, we see a different picture. The standard deviation of MSS between *P. troglodytes* and *P. paniscus* is 96.7%, with a variance of 1.8%. Despite their reproductive and morphological differences, chimpanzees and bonobos can hybridize in captivity (Vervaecke and Van Elsacker, 1992), and there is evidence of introgression of a small portion of nuclear genetic material between the two species based on a study of 75 wild-born chimpanzees and bonobos (de Manuel et al., 2016). The standard deviation of the MSS of

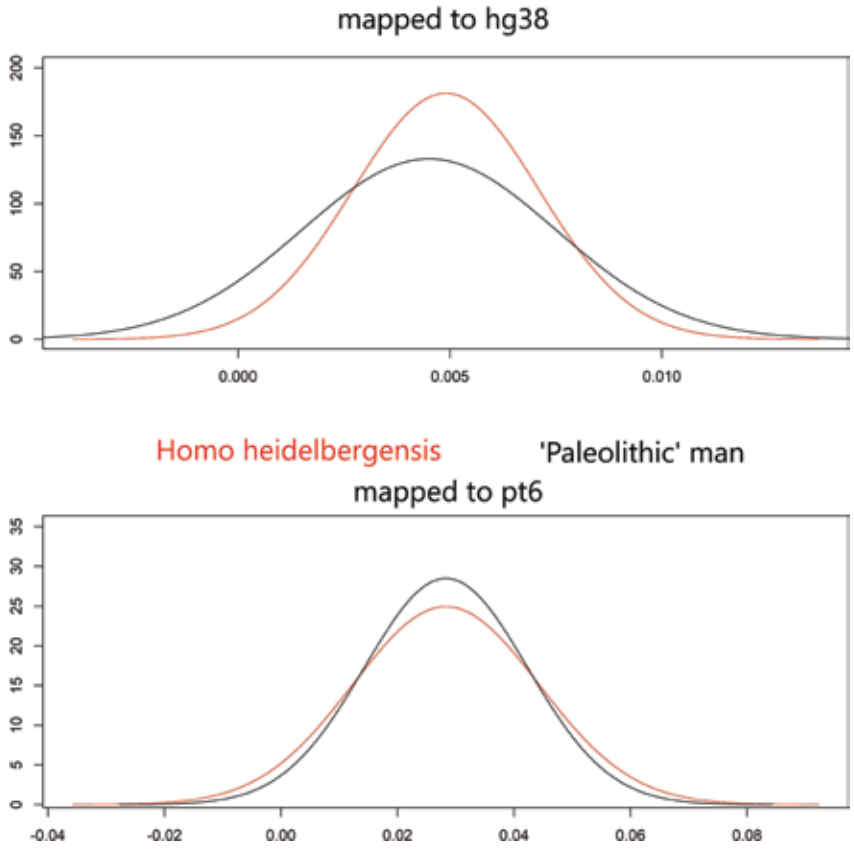

Figure 5. Normal distribution of mismatches between the first 10,000 read sequences from the nine PRJEB10957 and ten PRJEB22952 SRA samples mapped to hg38 and pt6. The red curve corresponds to *H. heidelbergensis*, whereas the black curve corresponds to 'paleolithic' archaic human.

Table I. Mean sequence similarity value between modern humans, Neanderthal, Denisovan, *H. heidelbergensis*, and *Pan*.

Group	Mean ± st.dev.	No. comparisons
All modern humans	$0.997 \pm 1.7 \times 10^{-3}$	210
Modern humans and Neanderthal	$0.986 \pm 7 \times 10^{-4}$	21
Modern humans and Denisovan	$0.975 \pm 5 \times 10^{-4}$	21
Modern humans and *H. heidelbergensis*	$0.967 \pm 6 \times 10^{-4}$	21
Modern humans and *Pan*	$0.91 \pm 9 \times 10^{-4}$	63
All *Pan*	$0.971 \pm 2.5 \times 10^{-2}$	3
Pan versus Neanderthal	$0.912 \pm 6 \times 10^{-4}$	3
Pan versus Denisovan	$0.909 \pm 6 \times 10^{-4}$	3
Pan versus *H. heidelbergensis*	$0.898 \pm 1.2 \times 10^{-3}$	3

Homo seen in Figure 3A is only around 0.9%, almost only half of that within *Pan*. Modern humans, Neanderthals, and Denisovans are thought to have interbred with one another in the past (Savanne, 2014; Pennisi, 2016; Rupe and Sanford, 2017). Furthermore, as we can see from Table I, the standard deviation of MSS between *H. heidelbergensis* and *Pan* is the least among *Homo*, at 89.8%. This indicates that *H. heidelbergensis* is the least similar to all other members of *Homo*. One might be misled to believe that *H. heidelbergenesis* is closest to *Pan* based on Figure 3A, but 3B clearly shows it is actually the least similar to *Pan* compared to other members of *Homo*. The mean MSS between *Pan* and all other Homo is 91%.

To illustrate relationships within the human holobaramin, a baraminic tree is presented in Figure 4. The 25 modern human individuals are closely grouped together, whereas Neanderthal, Denisovan, and *H. heidelbergensis* are more basal in the baraminic tree.

Variant Analysis of *H. heidelbergensis* and Modern Human

For each of the nine SRA samples from BioProject PRJEB10957 from *H. heidelbergensis*, several variant statistics were called, as reported in Table II. These same statistics are also provided for BioProject PRJEB22592 in Table III and are also available in Supplementary Data File 3.

Proportion of aligned reads to WGS

The proportion of aligned reads from a DNA sample to the WGS of another species should be high if the other genome comes from a species from the same holobaramin and lower if from another baramin. This is a qualitative measure only, for there is no absolute cutoff yet that one can use to determine if two species belong to separate kinds (Cserhati and Carter, 2020). Thus, the propor-

Table II. Variant calling statistics for PRJEB10957: reads from *H. heidelbergensis* to hg38, Neanderthal and pt6.

	% aln hg38	% aln ntal	% aln pt6	No. hg38 vars	hg38 var. density	No. ntal vars	ntal var. density	No. pt6 vars	pt6 var. density	pt6/ hg38 dens. prop.	pt6/ ntal dens. prop.	hg38/ ntal dens. prop.
Mean	0.966	0.959	0.742	16356.4	54.6	16904.556	51.1	35767.8	28.1	2.440	2.300	0.946
Std. dev.	0.034	0.035	0.161	32127.7	66.5	32951.654	62.2	59506.0	29.0	1.267	1.154	0.021

tion of reads from *H. heidelbergensis* mapping to hg38 and the proportion of reads from the archaic human to hg38 sample should not differ significantly. For PRJEB10957, the mean proportion of *H. heidelbergensis* reads mapping to hg38 (96.6±3.4%) is much higher than that mapping to pt6 (74.2±16.1%). This proportion is also very similar to the mean proportion of reads mapping to the Neanderthal genome (95.9±3.5%). This is noteworthy, since *H. heidelbergensis* is allegedly 1.3 Myr old, whereas Neanderthal is only 400 Kyr old according to the evolutionary timescale. Yet, these *H. heidelbergensis* reads are more similar to the sequence of the modern human genome than to the Neanderthal genome.

When comparing the proportion of reads mapping from *H. heidelbergensis* to hg38 to the proportion of the same reads mapping to pt6, there is a statistically significant difference, with a p-value of 0.003. When comparing the proportion of reads mapping from *H. heidelbergensis* to the Neanderthal WGS to the proportion of the same reads mapping to pt6, the p-value is 0.004.

However, when the proportion of *H. heidelbergensis* reads mapping to hg38 is compared to the proportion of these reads mapping to the Neanderthal WGS, the p-value is insignificant at 0.675. From this we can infer that the *H. heidelbergensis* reads map in the same manner to both modern (hg38) and the archaic genome (Neanderthal); there is no statistically significant difference between the two modes of mapping. This also indicates that *H. heidelbergensis* is just as human as both modern humans and Neanderthal.

Skewed variant frequency

The results presented here must be taken with caution, since sequencing aDNA does have its caveats. These include contamination with DNA from microbes or modern humans, and degradation of the aDNA (Thomas and Tomkins, 2014).

Proportionately slightly less *H. heidelbergensis* reads map to the hg38 genome, compared to reads from ancient ("Paleolithic") humans. Also, there are relatively more variants when mapping *H. heidelbergensis* reads to hg38 as opposed to ancient human reads (see Tables II and III). There are two reasons for this. The first is that DNA variants could have accumulated in the modern human genome over time, compared to the ancient genome of *H. heidelbergensis*. The second could be due to deamination from C to T (mirrored on the reverse strand as G to A). The research group that isolated the DNA from the *H. heidelbergensis* samples claims that the frequency of C>T deaminations rose from 12–17% at the 5' end of the reads to 55–62% at the 3' end of the reads (Meyer et al., 2014)! They found that

Table III. Variant calling statistics for PRJEB22592: reads from an *archaic human* to hg38, Neanderthal and pt6 (with USER treatment).

	% aln hg38	% aln ntal	% aln pt6	No. hg38 vars	hg38 var. density	No. ntal vars	ntal var. density	No. pt6 vars	pt6 var. density	pt6/ hg38 dens. prop.	pt6/ ntal dens. prop.	hg38/ ntal dens. prop.
Mean	0.999	0.996	0.945	2521616	70.737	2975644	59.190	20786182	8.211	74.870	1.180	0.847418
Std. dev.	0.000	0.001	0.006	1066303	58.051	1322310	46.696	11109092	5.688	2.081	1.240	0.806394

this rate of deamination is also similar to the same rate as found in bear remains from the same site at Sima de los Huesos. However, when doing the bioinformatics analysis, it is almost certain that they would have trimmed the edges of these reads where deamination could have been high.

The frequency of each of the twelve possible SNPs (when looking at all of the possible combinations between the four bases A, C, G, and T) was counted for each of the nine *H. heidelbergensis* SRA samples when mapped to both the hg38 and the Neanderthal genomes. This information can be found in Supplementary File 3. The proportion of each of the twelve SNPs between the *H. heidelbergensis* reads and both hg38 and the Neanderthal genome for SRA samples ERR995367–ERR995361 were plotted and can be found in Supplementary Figures 1a and b online. These five SRA samples were chosen, because the other four samples had a very low number of reads, and some of the twelve SNPs did not occur in those samples. The most common SNPs are C/T->G/A, making up 33.2%–47% for hg38 and 33.1–46.7% for Neanderthal. These high proportions cannot be by mere chance.

Guo and Jamison (2005) calculated that about 33.2% of all SNPs are C>T/G>A. The present study also calculated the frequency of C>T/G>A substitutions from the dbSNP to be 32%. The average C>T/G>A substitution rate over the five *H. heidelbergensis* SRA samples is 40.1±2.9%. Thus, the proportion of C>T/G>A substitutions between the *H. heidelbergensis* and modern human genomes is slightly elevated. This corresponds to a Z-score of 2.69, which denotes that the two distributions are significantly different. It suggests that around 6.9% of the C>T/G>A transitions are due to deamination.

The mean number and standard deviation of SNPs excluding C>T and G>A were calculated for these five samples (see "PRJEB10957 SNP hg38 dist." tab, rows "z (C>T)" and "z (G>A)" in Supplementary File 3). A z-score was calculated for C>T and G>T in these five samples to see how extreme they are. For all five samples the z-score was greater than 1.65, meaning that these results are significant at the 5% level. This means that the higher number of C>T and G>A variants are not occurring by random chance. Since the number of C>T and G>A variants are skewed, the genetic distance between *H. heidelbergensis* and modern humans decreases. It also strengthens the conclusion that *H. heidelbergensis* belongs to the human holobaramin.

Table IV. Mean % ± std. dev dissimilarity of 10,000 sequencing reads from SRA samples PRJEB10957 and PRJEB22952 mapped to hg38 and pt6.

	hg38	pt6
Homo heidelbergensis	0.0049±0.0022	0.0283±0.016
'Paleolithic' archaic human	0.0045±0.0030	0.0283±0.014
Z-score	0.108	1.9E-4

Percent dissimilarity of reads mapped to hg38 and pt6

Finally, the first 10,000 read sequences from the fastq file of the samples from PRJEB10957 and PRJEB22952 were mapped to both the hg38 and the pt6 genomes using BLASTN. The mean percent mismatches were noted as well as their standard deviations. The normal curves with these mean and standard deviation values are plotted in Figure 5, and the concrete mean and standard deviations are shown in Table IV. The z-score describes how similar two normal distributions are. Both values listed in the last row of Table IV show that the z-scores comparing *H. heidelbergensis* to hg38 and pt6 and also the 'paleolithic' archaic human to hg38 and pt6 are well below 2.0, meaning that these distributions are almost identical to one another. From this we can conclude that the genetic distance via read sequence mismatches between modern human and 'paleolithic' archaic human and between modern human *H. heidlbergensis* is virtually the same, supporting the idea that *H. heidelbergensis* is human.

Summary and Conclusion

From these analyses, we have seen that *H. heidelbergensis* behaves genetically similarly to modern and archaic humans. Its mtDNA sequence is only slightly different, being an archaic human. *H. heidelbergensis* clusters together with modern humans, Neanderthal, and Denisovan in the baraminogram (heatmap), as well as the baraminic tree, albeit at the base.

When nuclear data is examined in the form of SRA reads, about the same proportion of *H. heidelbergensis* reads map to the genomes of modern humans. A similar inference can be made when examining the average sequence mismatch between read sequences from *H. heidelbergensis* and archaic humans when mapped to hg38 and pt6.

All of these considerations confidently support placing *H. heidelbergensis* within the human holobaramin and are in concordance with prior studies on their morphological characteristics. This study nicely complements previous baraminology studies of this fossil human.

This study also highlights the utility of using aDNA from fossil humans in order to determine their baraminic placement. Here the mtDNA from only

four human subgroups were compared, but if genomes from more fossils could be isolated, such as *Homo erectus*, *Homo naledi*, *Homo floresiensis*, and others, this would sharpen the picture of human baraminic relationships even further.

Acknowledgments

The work in this paper was performed as a part of Creation Research Society grant #68. The author would like to thank Dr. Jeffrey Tomkins of the Institute for Creation Research for discussion on using blastn to compare mismatches when mapping read sequences to the genomes of human and chimpanzee.

References

Cserhati, M. 2022. Molecular baraminology of primates. *Creation Research Society Quarterly* 59(2):72–80.

Cserhati, M., and R.W. Carter. 2020. Hierarchical clustering complicates baraminological analysis. *Journal of Creation* 34(3): 41–50.

Cserhati, M.F., M.E. Mooter, L. Peterson, B. Wicks, P. Xiao, M. Pauley, and C. Guda, 2018. Motifome comparison between modern human, Neanderthal, and Denisovan. *BMC Genomics* 19(1): 472.

de Manuel, M., M. Kuhlwilm, P. Frandsen, V.C. Sousa, T. Desai, J. Prado-Martinez, J. Hernandez-Rodriguez et al. 2016. Chimpanzee genomic diversity reveals ancient admixture with bonobos. *Science* 354(6311): 477–481.

Guo, Y., and D.C. Jamison. 2005. The distribution of SNPs in human gene regulatory regions. *BMC Genomics* 6: 140.

Kumar, S., G. Stecher, M. Li, C. Knyaz, and K. Tamura K. 2018. MEGA X: Molecular Evolutionary Genetics Analysis across computing platforms. *Molecular Biology and Evolution* 35: 1547–1549.

Line, P. 2013. Explaining robust humans. *Journal of Creation* 27(3): 64–71.

Lubenow, M.L. 2004. *Bones of Contention: A Creationist Assessment of Human Fossils*, 2nd edition. Baker Books, Grand Rapids, Michigan.

Meyer, M., Q. Fu, A. Aximu-Petri, I. Glocke, B. Nickel, J.L. Arsuaga, I. Martínez, A. Gracia, J.M. de Castro, E. Carbonell, and S. Pääbo. 2014. A mitochondrial genome sequence of a hominin from Sima de los Huesos. *Nature* 505(7483): 403–406.

Pennisi, E. 2013. Human evolution: More genomes from Denisovan cave show mixing of early human groups. *Science* 340: 799.

Poullet, M., and L. Orlando. 2020. Assessing DNA sequence alignment methods for characterizing ancient genomes and methylomes. *Frontiers in Ecology and Evolution* 8(105).

Rupe, C., and L. Sanford. 2017. *Contested Bones*. FMS Publications, Waterloo, NY.

Saitou, N., and M. Nei. 1987. The neighbor-joining method: A new method for reconstructing phylogenetic trees. *Molecular Biology and Evolution* 4: 406–425.

Savanne, D. 2014. Denisovans menace evolution—A new chapter in the human origins debate. *Journal of Creation* 28(3): 5–8.

Schubert, M., L. Ermini, C. Der Sarkissian, H. Jónsson, A. Ginolhac, R. Schaefer, M.D. Martin et al. 2014. Characterization of ancient and modern genomes by SNP detection and phylogenomic and metagenomic analysis using PALEOMIX. *Nature Protocols* 9(5): 1056–1082.

Sikora, M., A. Seguin-Orlando, V.C. Sousa, A. Albrechtsen, T. Korneliussen, A. Ko et al. 2017. Ancient genomes show social and reproductive behavior of early upper paleolithic foragers. *Science* 358: 659–662.

Tamura, K., M. Nei, and S. Kumar. 2004. Prospects for inferring very large phylogenies by using the neighbor-joining method. *Proceedings of the National Academy of Sciences (USA)* 101: 11030–11035.

Thomas, B., and J. Tomkins. 2014. How reliable are genomes from ancient DNA? *Journal of Creation* 28(3): 92–98.

Tomkins, J. 2015. Documented anomaly in recent versions of the BLASTN algorithm and a complete reanalysis of chimpanzee and human genome-wide DNA similarity using Nucmer and LASTZ. *Answers Research Journal* 8: 379–390.

Tomkins, J. 2018. Comparison of 18,000 de novo assembled chimpanzee contigs to the human genome yields average BLASTN alignment identities of 84%. *Answers Research Journal* 11: 215–219.

Vervaecke, H., and L. Van Elsacker. 1992. Hybrids between common chimpanzees (*Pan troglodytes*) and pygmy chimpanzees (*Pan paniscus*) in captivity. *Mammalia* 56: 667–669.

Wood, B., and M. Collard. 1999. The human genus. *Science* 284(5411): 65–71.

Wood, T.C. 2010. Baraminological analysis places *Homo habilis*, *Homo rudolfensis*, and *Australopithecus sediba* in the human holobaramin. *Answers Research Journal* 3: 71–90.

Woodmorappe, J. 1999. The non-transitions in 'human evolution'—on evolutionists' terms. *Journal of Creation* 12(2): 10–12.